

Ultrafast inhomogeneous magnetization dynamics analyzed by interface-sensitive nonlinear magneto-optics

J. Chen,¹ J. Wieczorek,¹ A. Eschenlohr,^{1, a)} S. Xiao,¹ A. Tarasevitch,¹ and U. Bovensiepen¹

Faculty of Physics and Center for Nanointegration (CENIDE), University of Duisburg-Essen, Lotharstr. 1, 47057 Duisburg, Germany

(Dated: 5 September 2018)

We analyze laser-induced ultrafast, spatially inhomogeneous magnetization dynamics of epitaxial Co/Cu(001) films in a 0.4-10 nm thickness range with time-resolved magnetization-induced second harmonic generation, which probes femtosecond spin dynamics at the vacuum/Co and Co/Cu interfaces. The interference of these two contributions makes the overall signal particularly sensitive to differences in the transient magnetization redistribution between the two interfaces, i.e. ultrafast magnetization profiles in the ferromagnetic film. We find in films of up to 3 nm thickness a stronger demagnetization at the surface, because the film thickness is smaller than the effective mean free path of the spin current mediating the demagnetization, i.e. the difference between the mean free paths of the majority and minority carriers. For film thicknesses larger than 3 nm, the magnetization profile reverses, since majority spins can escape into the conducting substrate only from the interface-near region.

PACS numbers: 72.25.Ba, 72.25.Fe, 72.25.Mk, 75.78.Jp, 78.20.Ls

The observation of optically excited ultrafast spin currents in ferromagnetic (FM) metals^{1,2} has opened up new possibilities to manipulate magnetization on sub-picosecond timescales. Both transient magnetization enhancement³ and ultrafast demagnetization^{4,5} by such spin-dependent, screened⁶ charge currents, as well as spin-transfer torque⁷ in metallic layered structures, were recently demonstrated. These discoveries make it conceivable to extend spintronics into the ultrafast regime, employing highly excited, non-equilibrium spin-polarized carriers. In this context, analyzing spin dynamics at interfaces has become increasingly important, as the interface properties are decisive for spin transport in heterostructures potentially relevant for applications, e.g. employing spin valves or multilayers^{8,9}. An experimental technique capable of addressing this issue must be interface sensitive, as well as able to probe spin dynamics at buried interfaces, on the relevant fs timescales in a pump-probe experiment.

Here, we show that magnetization-induced second harmonic generation (mSHG)¹⁰ can probe and even distinguish contributions to spin dynamics from several interfaces in a ferromagnet-metal heterostructure by performing a fs time-resolved, thickness-dependent study on epitaxial Co/Cu(001) films as a model system. Based on this analysis, we identify transient spatial magnetization profiles in the direction normal to the sample surface during ultrafast demagnetization. We find that these profiles reflect the effective escape depth of fs spin currents into Cu via the difference in the spin-dependent mean free paths (MFP) of majority and minority electrons, thus changing strongly with increasing sample thickness.

The schematic experimental arrangement is depicted

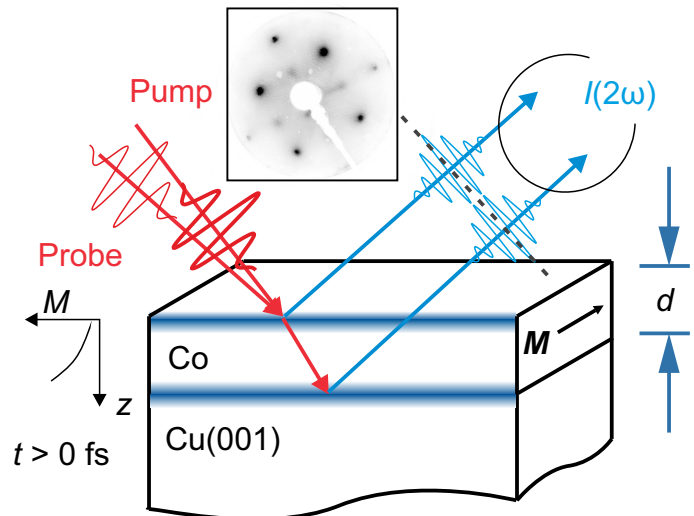


FIG. 1. Schematic experimental setup for measuring the interface-sensitive mSHG yield in reflection from Co/Cu(001) for different Co film thicknesses d ranging from 0.4 nm to 10 nm in a pump-probe experiment. Ultrafast demagnetization due to the pump pulse will lead to a spatially inhomogeneous change in the magnetization M along the film depth z ¹¹. (inset) LEED pattern at 128 eV kinetic energy of 0.9 nm thick Co/Cu(001), showing the four-fold symmetry expected from epitaxial growth of Co.

in Fig. 1. Ultrashort laser pulses were generated from a cavity-dumped Ti:Sa oscillator, with a pulse width of 35 fs at a central wavelength of 800 nm, 40 nJ pulse energy and a repetition rate of 2.53 MHz. The pump and probe beams were split at a 4:1 intensity ratio. The incident pump fluence at the sample surface was 6 mJ/cm², and the pump pulses were s-polarized. We measured the reflected second harmonic (SH) yield at 400 nm wavelength from the sample, using a BG39 optical filter and a

^{a)}andrea.eschenlohr@uni-due.de; www.uni-due.de/agbovensiepen

grating monochromator, by single photon counting. The measurements were performed in the transversal geometry, i.e. with the magnetization M aligned in the sample plane and normal to the optical plane of incidence by an applied magnetic field large enough to reverse M . The ingoing probe pulse was p-polarized, and p-polarized SH radiation was detected in the static experiments. In the pump-probe experiments, detection was performed without polarization analysis. Co films with thicknesses $0.4 \text{ nm} \leq d \leq 10 \text{ nm}$ were grown *in situ* by electron beam evaporation in ultrahigh vacuum ($< 10^{-10} \text{ mbar}$) on a Cu(001) single crystal prepared by sputtering-annealing cycles¹². Epitaxial growth was verified by low energy electron diffraction (LEED), see Fig. 1.

Essential for the interpretation of our time-resolved mSHG results is the fact that the overall detected SH radiation is generated at two interfaces, namely vacuum/Co and Co/Cu, in our Co/Cu(001) samples, see Fig. 1, and that the respective magnetization-dependent SH fields interfere with each other. We will first discuss the static thickness dependence, which allows us to describe this interference.

The magnetization-dependent SH field $|E_{\text{odd}}| \cdot \cos(\alpha) \approx \frac{I^{\uparrow} - I^{\downarrow}}{4|E_{\text{even}}|}$, with the magnetization-independent SH field $|E_{\text{even}}| \approx \sqrt{\frac{I^{\uparrow} + I^{\downarrow}}{2}}$, is determined from the measured SH intensities $I^{\uparrow, \downarrow}$ at opposite orientations of M . Its thickness dependence for $0.4 \text{ nm} \leq d \leq 10 \text{ nm}$ is displayed in Fig. 2. Here, α refers to the phase between $|E_{\text{even}}|$ and $|E_{\text{odd}}|$, which is close to zero and constant for small d ¹³. We thus assume $\alpha = 0$ in the following. $|E_{\text{odd}}|$ decreases sharply until about $d = 3 \text{ nm}$, then increases before staying at nearly constant values for larger d . In order to explain this behavior, we will describe E_{odd} in terms of the contributions from the Co surface $E_{\text{odd}}^{\text{S}}$ and the Co/Cu interface $E_{\text{odd}}^{\text{I}}$, i.e. $E_{\text{odd}} = E_{\text{odd}}^{\text{S}} + E_{\text{odd}}^{\text{I}}$, where $E_{\text{odd}}^{\text{S}} = a_{\text{S}} \cdot m_{\text{S}} \cdot E_{\omega, \text{S}}^2$ and $E_{\text{odd}}^{\text{I}} = a_{\text{I}} \cdot m_{\text{I}} \cdot E_{\omega, \text{I}}^2 \cdot U(d)$, with m_{S} and m_{I} being the magnetization, and $E_{\omega, \text{S}}$ and $E_{\omega, \text{I}}$ the electric field of the fundamental pulse, at the surface respectively the interface. The proportionality factors a_{S} and a_{I} are given by the Fresnel factors and the symmetry-allowed magnetization-dependent elements of the second-order nonlinear susceptibility tensor¹⁴. $U(d)$ describes the damping and phase shift of the SH field generated by the Co film. Consequently, mSHG preferentially probes the surface contribution with increasing d , because the SH from the interface is increasingly damped. Moreover, additional effects can occur due to interference of the surface and phase-shifted interface contributions. We combine the above to an effective description with

$$|E_{\text{odd}}(d)| = \left| A_{\text{odd}}^{\text{S}} + A_{\text{odd}}^{\text{I}} \cdot e^{-1.29\beta d} \cdot e^{i(0.017\varphi + 0.077d)} \right|, \quad (1)$$

where $A_{\text{odd}}^{\text{S}} = a_{\text{S}} \cdot E_{\omega, \text{S}}^2$, $A_{\text{odd}}^{\text{I}} = a_{\text{I}} \cdot E_{\omega, \text{I}}^2$, β the effective damping in Co and φ the effective relative phase shift between the surface and interface contributions, and fit our static mSHG data, see Fig. 2. The resulting value is $\varphi = 186 \pm 8^\circ$, showing a destructive interference of

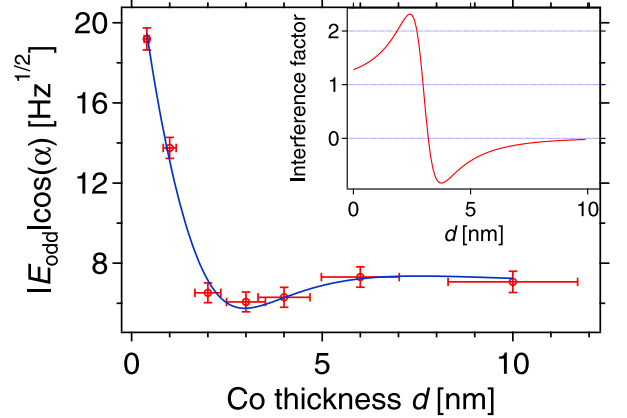


FIG. 2. Static measurement (circles) of the odd part of the SH field depending on the Co film thickness d . The solid line is a fit to the data according to equation 1. The inset depicts the calculated interference factor $\text{int}(d)$ between the odd contributions from the vacuum/Co and the Co/Cu interfaces.

the surface and interface contributions. The value of $\varphi \approx 180^\circ$ occurs due to the incident beam being reflected at the FM layer at the vacuum/Co interface, and conversely at Cu after propagating through Co, in agreement with earlier findings¹⁵.

Now, we turn our attention to the time-resolved mSHG response, shown in Fig. 3 (top). Δ_{odd} stands for the pump-induced relative change of $|E_{\text{odd}}| \cdot \cos(\alpha)$, normalized to its value before laser excitation. It is obvious that at various thicknesses, Δ_{odd} shows distinctively different behavior. For $d = 0.4 \text{ nm}$, which equals two monolayers, a negative change of Δ_{odd} occurs in the first few tens of fs after laser excitation, as expected for ultrafast demagnetization of the Co film, before a slower relaxation back to the equilibrium value. However, Δ_{odd} for $2 \text{ nm} \leq d \leq 4 \text{ nm}$ shows a positive change. For $d \geq 6 \text{ nm}$, a sign change in the transient response occurs. We argue that this time- and d -dependent behavior is caused by spatially inhomogeneous magnetization dynamics in the FM film, which can in particular occur due to laser-induced spin transport and spin-flip scattering^{2,6,11}. Since E_{odd} is very sensitive to differences between m_{S} and m_{I} due to the destructive interference of the SH fields from the two interfaces, our experiment is particularly sensitive to such effects.

To substantiate that the evolution of Δ_{odd} is given by the transient relative changes of the magnetization at the interface $\Delta m_{\text{I}} = (m_{\text{I}}/m_{\text{I}}(t < 0)) - 1$ and the surface $\Delta m_{\text{S}} = (m_{\text{S}}/m_{\text{S}}(t < 0)) - 1$, we approximate our time-dependent data as follows. As discussed above, the mSHG signal is dominated by the interface at low d and the surface at higher d . Therefore, we take $\Delta_{\text{odd}}(10 \text{ nm})$ and $\Delta_{\text{odd}}(0.4 \text{ nm})$ as approximations of $\Delta_{\text{odd}}^{\text{S}}$ and $\Delta_{\text{odd}}^{\text{I}}$, respectively. It should thus be possible to describe the experimental data with a linear combination of the two

terms,

$$\Delta_{\text{odd}}(d) = a\Delta_{\text{odd}}(10 \text{ nm}) + b\Delta_{\text{odd}}(0.4 \text{ nm}), \quad (2)$$

where a and b represent the respective contributions from surface and interface, which change with thickness. As shown in Fig. 3 (bottom) for intermediate d , the linear combination of $\Delta_{\text{odd}}(10 \text{ nm})$ and $\Delta_{\text{odd}}(0.4 \text{ nm})$ agrees well with the experimental data for $0.4 \text{ nm} < d < 10 \text{ nm}$ at short delays up to about 0.5 ps. Only at longer delays, when the hot electron population thermalizes with the lattice, a deviation can be found. This agreement supports our assumption of interfering interface contributions also for dynamic, laser-induced changes, at least until lattice heating sets in. The thickness dependence of $|b|/(|a| + |b|)$, see Eq. 2, is displayed in Fig. 4 (left). It clearly shows a continuous decrease of the interface contribution to Δ_{odd} with increasing d , as expected.

In order to analyze the transient magnetization profiles^{2,6,11}, we approximate Δ_{odd} in terms of Δm_S and Δm_I in first order as

$$\Delta_{\text{odd}}(t, d) \approx \Delta m_S(t) + \text{int}(d) \cdot (\Delta m_I(t) - \Delta m_S(t)). \quad (3)$$

We term $\text{int}(d)$ the interference factor, which determines how transient magnetization profiles, i.e. differences in Δm_S and Δm_I , are expressed in Δ_{odd} for a certain d . The interference factor describes the relative contribution of the damped and 180° phase-shifted SH from the interface to the overall signal. It is calculated as $\text{int}(d) = \Re(B_{\text{odd}}^I(d)/(A_{\text{odd}}^S + B_{\text{odd}}^I(d))$ from the fit results according to Eq. 1, with $B_{\text{odd}}^I(d)$ referring to the second term on the right hand side of Eq. 1, and displayed in the inset of Fig. 2. The d -dependent changes in $\Delta_{\text{odd}}(t)$ shown in Fig. 3 (top) can now be understood with the aid of Eq. 3: The expected negative change due to demagnetization can be more than compensated by a difference in the amount of demagnetization between surface and interface, which enters the observed signal via $\text{int}(d)$. In order to illustrate how mSHG probes magnetization profiles $\Delta m_I - \Delta m_S$, we rewrite equation 3 as

$$\Delta m_I(t) - \Delta m_S(t) \approx (\Delta_{\text{odd}}(t) - \Delta m_{av}(t))/(int(d) - 0.5), \quad (4)$$

with Δm_{av} referring to the average relative magnetization change in the film. We can thus calculate $\Delta m_I - \Delta m_S$, provided we have an observable for Δm_{av} . For $d \leq 4 \text{ nm}$, the transversal magneto-optical Kerr effect (T-MOKE) acquired simultaneously with the mSHG is shown in Fig. 4. It has a rather uniform depth sensitivity¹⁶ and therefore serves as a good approximation for $\Delta m_{av}(t)$.

From the results of the calculation according to equation 4, shown in Fig. 4 (right) for 2 and 4 nm thickness, we see that for $d \leq 3 \text{ nm}$ $|\Delta m_S| > |\Delta m_I|$, while for $d \geq 4 \text{ nm}$ $|\Delta m_S| < |\Delta m_I|$ and thus $\Delta m_I - \Delta m_S$ reverses. We can conclude that the sign changes in $\Delta m_I - \Delta m_S$ are connected to the inelastic, spin-dependent electron MFP, if we consider that ultrafast demagnetization

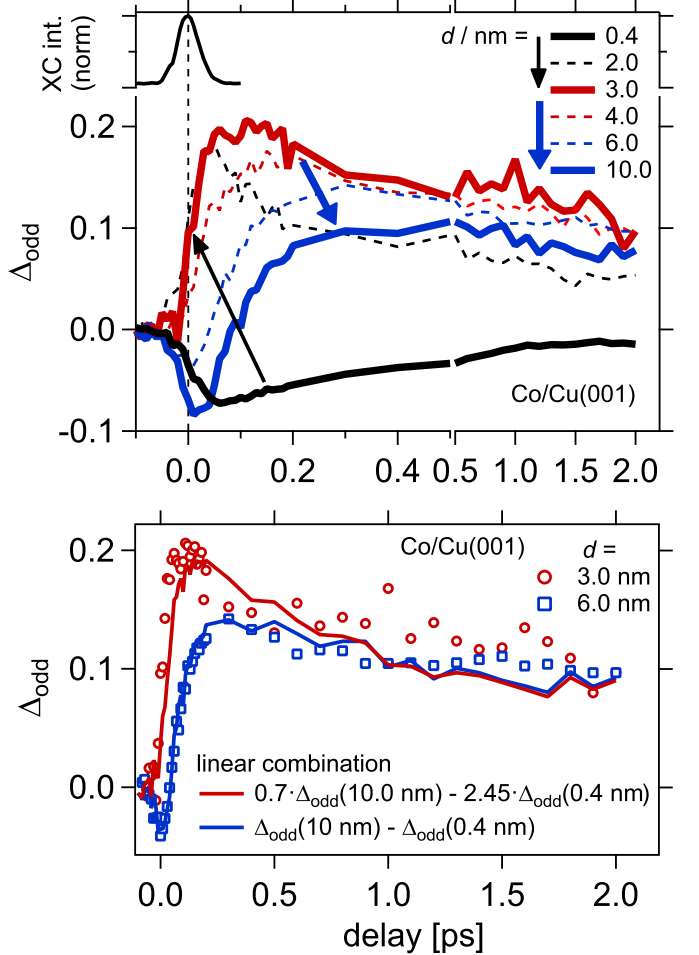


FIG. 3. (top) Time-resolved mSHG data $\Delta_{\text{odd}}(t, d)$ versus the pump-probe time delay. The pump-probe cross-correlation (XC) indicates the experimental time resolution. Arrows indicate the evolution of the time-dependent $\Delta_{\text{odd}}(t, d)$ signal with increasing thickness d . (bottom) Modelling of $\Delta_{\text{odd}}(d)$ by linear combinations of $\Delta_{\text{odd}}(0.4 \text{ nm})$ and $\Delta_{\text{odd}}(10 \text{ nm})$ (lines) as described in the main text, in comparison to the experimental data (symbols).

of thin ferromagnetic films on conducting substrates is driven primarily by fs spin currents before electron thermalization occurs^{1,2,6,11}, i.e. majority spins escape into the substrate and cause a loss of spin polarization. For thicknesses which approach these MFPs of typically a few nm in the 3d transition metal ferromagnets^{17,18}, it becomes less likely that majority spins propagate from the surface into the substrate before scattering. Instead a spatially inhomogeneous demagnetization which is stronger in the region near the interface to the substrate, i.e. the spin current sink, occurs. This effect can also be enhanced by the fact the minority spins with lower MFPs compared to the majority spins^{17,18} cannot leave the Co films for larger d and accumulate near the buried interface⁵. Thus, the transient magnetization profiles are strongly influenced by the difference between the

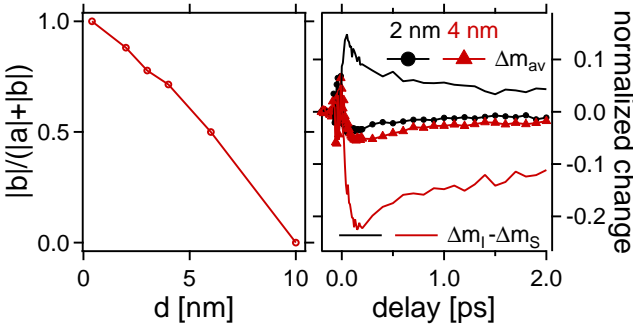


FIG. 4. (left) Ratio of the normalized linear combination factor $|b|$ over Co thickness. (right) Δm_{av} for $d = 2, 4$ nm Co/Cu(001) (symbols) together with $\Delta m_I - \Delta m_S$ calculated according to equation 4 (lines).

majority and minority electron MFPs. Our finding that the sign of $\Delta m_I - \Delta m_S$ reverses between $d = 3$ nm and $d = 4$ nm, compare Fig. 4 (right), is consistent with the minority electron MFP being approximately 1-2 nm¹⁷, while the majority electron MFP is a factor of about 1.2 to 3 larger in the relevant energy range of up to 1.5 eV above the Fermi level¹⁷⁻¹⁹.

For $d \geq 6$ nm, our analysis according to equation 4 is not suitable due to the fact that T-MOKE probes the demagnetization in an increasingly spatially inhomogeneous manner and does not provide a satisfactory approximation for Δm_{av} any more. However, the transient change shown for these d , compare Fig. 3 (top), is still consistent with our previous results on Co/Cu(001)¹¹, which show a transiently changing spatial magnetization gradient due to the interplay between spin transport and phonon-mediated spin-flip scattering. A change of the sign of Δ_{odd} , which is linked to a changing magnitude or sign of $\Delta m_I - \Delta m_S$, occurs at around 100 fs, i.e. the electron thermalization time at which the stronger demagnetization at the interface due to spin transport recedes and the surface-near region starts to demagnetize due to the now dominant spin-flip scattering¹¹.

Note that these results demonstrate that mSHG is sensitive to spatially inhomogeneous spin dynamics on lengthscales of a few nm, which is well below the optical penetration depth in the 3d transition metals of typically 10-20 nm responsible for the gradient in the initial laser excitation, and on the order of the spin-dependent electron MFPs^{17,18} governing spin transport. Here, mSHG can provide information about spatially inhomogeneous magnetization dynamics not available to bulk-sensitive probing via the depth sensitivity of MOKE, which is less pronounced at $d < 6$ nm^{11,16}.

In summary, we have demonstrated that mSHG serves as a sensitive probe for spatially inhomogeneous magnetization dynamics in epitaxial Co/Cu(001) films, due to interference of the contributions from the vacuum/Co

and Co/Cu interfaces, which make up the overall mSHG signal. At $d \leq 4$ nm, it probes the sign change of the transient magnetization profile with increasing d caused by the effective MFP of the fs spin current leading to demagnetization. At $d \geq 6$ nm, mSHG serves as a probe of transient magnetization profiles complementary to linear bulk-sensitive time-resolved magneto-optical measurements¹¹. This demonstrates the strength of mSHG as a probe for spatially inhomogeneous magnetization dynamics, e.g. due to spin currents in a conducting heterostructure with several interfaces.

ACKNOWLEDGMENTS

This work was funded by the German Research Foundation (DFG) through SPP 1840 QUTIF, Grant No. ES 492/1-1, and by Mercator Research Center Ruhr (MERCUR), Grant No. Pr-2014-0047.

- ¹M. Battiato, K. Carva, and P. M. Oppeneer, Phys. Rev. Lett. **105**, 027203 (2010).
- ²A. Melnikov, I. Razdolski, T. O. Wehling, E. Th. Papaianou, V. Roddatis, P. Fumagalli, O. Aktsipetrov, A. I. Lichtenstein, and U. Bovensiepen, Phys. Rev. Lett. **107**, 076601 (2011).
- ³D. Rudolf *et al.*, Nat. Commun. **3**, 1037 (2012).
- ⁴G. Malinowski, F. Dalla Longa, J. H. H. Rietjens, P. V. Paluskar, R. Huijink, H. J. M. Swagten, and B. Koopmans, Nat. Phys. **4**, 855-858 (2008).
- ⁵A. Eschenlohr, M. Battiato, P. Maldonado, N. Pontius, T. Kachel, K. Holldack, R. Mitzner, A. Föhlisch, P. M. Oppeneer, and C. Stamm, Nat. Mater. **12**, 332-336 (2013).
- ⁶M. Battiato, K. Carva, and P. M. Oppeneer, Phys. Rev. B **86**, 024404 (2012).
- ⁷A. J. Schellekens, K. C. Kuiper, R. R. J. C. de Wit, and B. Koopmans, Nat. Commun. **5**, 4333 (2014).
- ⁸P. Beliën, R. Schad, C. D. Potter, G. Verbanck, V. V. Moshchalkov, and Y. Bruynsraede, Phys. Rev. B **50**, 9957-9962 (1994).
- ⁹P. Zahn, J. Binder, I. Mertig, R. Zeller, and P. H. Dederichs, Phys. Rev. Lett. **80**, 4309-4312 (1998).
- ¹⁰R.-P. Pan, H. D. Wei, and Y. R. Shen, Phys. Rev. B **39**, 1229-1234 (1989).
- ¹¹J. Wieczorek, A. Eschenlohr, B. Weidtmann, M. Rösner, N. Bergeard, A. Tarasevitch, T. O. Wehling, and U. Bovensiepen, Phys. Rev. B **92**, 174410 (2015).
- ¹²L. Gonzalez, R. Miranda, M. Salmeron, J. A. Verges, and F. Yndurain, Phys. Rev. B **24**, 3245-3254 (1981).
- ¹³U. Conrad, J. Gütte, V. Jähnke, and E. Matthias, Phys. Rev. B **63**, 144417 (2001).
- ¹⁴W. Hübner, K. H. Bennemann, and K. Böhmer, Phys. Rev. B **50**, 17597-17605 (1994).
- ¹⁵H. A. Wierenga, M. W. J. Prins, D. L. Abraham, and Th. Rasing, Phys. Rev. B **50**, 1282-1285 (1994).
- ¹⁶A. Eschenlohr, J. Wieczorek, J. Chen, B. Weidtmann, M. Rösner, N. Bergeard, A. Tarasevitch, T. O. Wehling, and U. Bovensiepen, Proc. SPIE **9746**, Ultrafast Phenomena and Nanophotonics XX, 97461E (2016).
- ¹⁷V. P. Zhukov, E. V. Chulkov, and P. M. Echenique, Phys. Rev. B **73**, 125105 (2006).
- ¹⁸S. Kaltenborn and H. C. Schneider, Phys. Rev. B **90**, 201104(R) (2014).
- ¹⁹A. Goris, K. M. Döbrich, I. Panzer, A. B. Schmidt, M. Donath, and M. Weinelt, Phys. Rev. Lett. **107**, 026601 (2011).